Gravitational Constant (*G*) in Measurements

Kiyoung Kim†

Abstract

In the late 1990s, scientists recognized that the universal gravitational constant (*G*) could not be measured as precisely as other physical constants; even today, the precise measurement of *G* remains a profound challenge in physics. However, this difficulty may be explained by a new paradigm of physics in which physical mass and electric charges interact, meaning fundamental forces like gravity and electromagnetism cannot exist independently. Consequently, variations in *G* measurements appear to coincide with fluctuations in both the Earth's geomagnetic field and the Length of Day (LOD). Specifically, geomagnetic variations are initiated by interactions with the primitive virtual negative (PVN) charges of other planets in the solar system, while LOD fluctuations follow due to Faraday's law of induction acting on these geomagnetic variations; ultimately, these geomagnetic field variations drive the changes in *G* measurements.

† kkim.pvn@gmail.com

Introduction

For nearly three decades, it has been known that the universal gravitational constant, or "Big *G*," cannot be reliably measured beyond three decimal places. Despite intensive efforts to achieve greater precision, scientists remain puzzled; not only has measurement accuracy failed to improve, but the values obtained in worldwide experiments also remain inconsistent beyond their stated uncertainties. Consequently, Big *G* remains the "black sheep" of fundamental constants. (physicsworld 2001, Johnston 2018, NIST 2026, Schlamminger, Chao, et al. 2026)

In the meantime, an interesting 2015 report suggested that Big *G* measurements might be closely related to changes in Earth's rotation rate—specifically the Length of Day (LOD)—which fluctuates on the order of milliseconds and exhibits a 5.9-year periodicity (Anderson, et al. 2015). However, a subsequent investigation by Schlamminger et al. (2015) found that measured *G* values do not show a significant periodic variation; thus, the correlation to LOD is doubtful. In addition, they hypothesized that the variation of *G* values in these measurements stems from as-yet-unknown systematic offsets and errors. (Schlamminger, Gundlach and Newman 2015)

However, this "black sheep" status was confirmed once again when an American experiment failed to replicate the original findings from the Bureau International des Poids et Mesures (BIPM), despite a decade-long effort utilizing an identical setup. As shown in Table A and Figure A (Appendix A), the *G* values reported by the BIPM in 2001 and 2013 are mutually consistent, yet they differ significantly from the value reported by the US team in 2026.

Mainstream scientists believe that a strong physical correlation exists between geomagnetic field variance and LOD, but they maintain that there is absolutely no relation to the variance of *G* measurements. In addition, they consider the 5.9-year secular variation period of LOD and the orbital period of Jupiter around the Sun to be a mere numerical coincidence. On the other hand, several theories have been proposed to explain this discrepancy. Some attribute it to external interference, such as the solar cycle, the orbital period of Jupiter, or the alignment of the measuring device with Jupiter and the galaxy (Guynn 2021, Unnikrishnan). Other theories even hypothesize that the gravitational constant (*G*) is not truly constant but anisotropic, meaning it varies depending on direction (Gershteyn, et al. 2002). If the "ugly duckling" measurement anomaly of *G* can be resolved by a "black sheep" approach, it might be ironic.

First, we need to examine data from worldwide (*G*) measurements to understand how experimentally measured values vary depending on location and data acquisition times. Next, we will investigate any reasonable suspicions regarding what might affect these (*G*) measurements—known as unknown systematic errors. Finally, we explain the main reasons why the gravitational constant remains the least precise fundamental constant in physics.

Gravitational Constant (*G*) in Experiments

The gravitational constant *G* has been measured in laboratories worldwide. Table A in Appendix A lists Big G values measured from 1930 to 2026, which are shown in Figure A with *G* values recommended from CODATA (Committee on Data of International Science Council).

As shown in Figure A, the *G* values have not converged to a single value; instead, they exhibit fluctuations. This indicates that the precision of the experimentally measured *G* values has only three or four significant figures, which might result from unknown systematic environmental interferences. Before we investigate further, we need to check whether the fluctuations in *G* values exhibit a pattern or periodicity.

Interestingly, a unique experiment measuring the gravitational constant (*G*) lasted for 15 years at the same place in Russia (Karagioz and Izmailov 2001), which should be very important asset for the research of gravitational constant (*G*) measurements. Figure 1 shows the variation of *G* values measured from 1985 to 2000, in which type-A uncertainty is used for uncertainty of *G* values measured; since the "Series Number" in Table 1 indicates 'the beginning of that particular series of measurements', actual measurement date is considered as following.

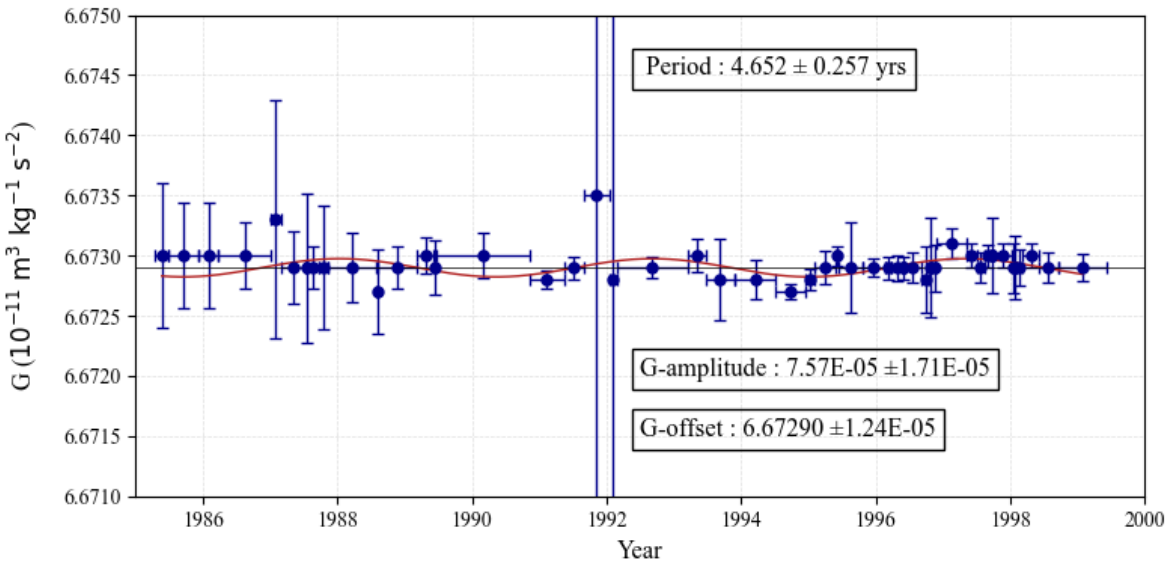

Figure 1: Data from Table1 *(Karagioz and Izmailov 2001)*

For example, as shown in the first row of Table 1, if a series of measurements started on 850419 and the second series started on 850629, the proper date for the first series is better to be represented by the midpoint between the two dates, along with its corresponding uncertainty, which is equal to half the time elapsed between them. Using Orthogonal Distance Regression (ODR) model in Python, 39 data points out of 40[‡] were fitted to a sinusoidal function, yielding a reduced chi-squared (χ^2_{red}) value of 0.3909.

On the other hand, every four years, the Committee on Data of the International Science Council (CODATA) recommends an updated value for the gravitational constant (*G*) based on the latest scientific measurements. Figure 2 shows *G* values measured in Russia as shown in Figure 1 and *G* values recommended by CODATA. Interestingly, G-offset is 6.6729×10^{-11}

[‡] In the 980605 series, the G value was anomalously measured as 6.730 for an unknown reason.

in Figure 1, which is remarkably close to the CODATA-recommendation value of 6.673×10^{-11} in 1998 as shown in Figure 2, in which "scipy.optimize.curv_fit" function from the SciPy library in Python was used. However, reduced chi-squared (χ^2_{red}) values for measured data (Karagioz and Izmailov 2001) and CODATA are 0.3845 and 0.0277, respectively.

In both figures, the reduced chi-squared values ($\chi^2_{red} < 1.0$ and χ^2_{red}(CODATA) $\ll 1.0$) indicate either that the measurement errors were overestimated or that factors beyond simple systematic and random errors played a role. Moreover, although the gravitational constant (G) is supposed to be invariant—remaining constant at anytime and anywhere—it can exhibit dependency on location in experiments, just as it shows a dependency on time as shown above.

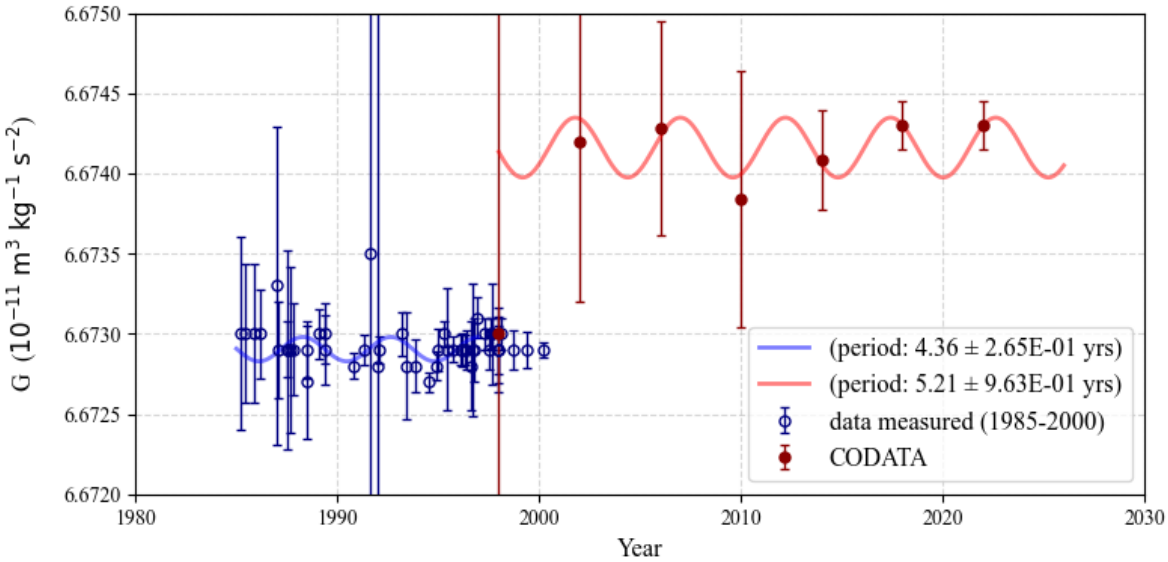

Figure 2: CODATA-recommendation values vs. years

For example, a periodic variation is clearly visible in Figure 3, where data were selected only from the USA-based experiments listed in Table A (Appendix A) and fitted to a sine function with $\chi^2_{red} = 1.4264$.

The data on the gravitational constant (G) measured from 1930 to 2026, presented in Table A and Figure A (Appendix A), yield several key insights. First, errors in G measurements do not arise from statistical random fluctuations, as demonstrated in Figures 1 and 2; this indicates the involvement of an as-yet-unknown external interference. In addition, this interference varies periodically, as illustrated in Figure 3, which reveals a period of 5.525 years (approximately half of a solar cycle). Moreover, this interference is not only time-dependent but also varies by geographic location.

Although we cannot pin down all the reasons for hidden systematic offsets and errors in experiments (dark uncertainty) and yet-unknown external interferences, we can posit that the major factor behind the variation of G values in measurements originates from the mass-charge interaction in the 4-D complex space model in physics (Kim 2008).

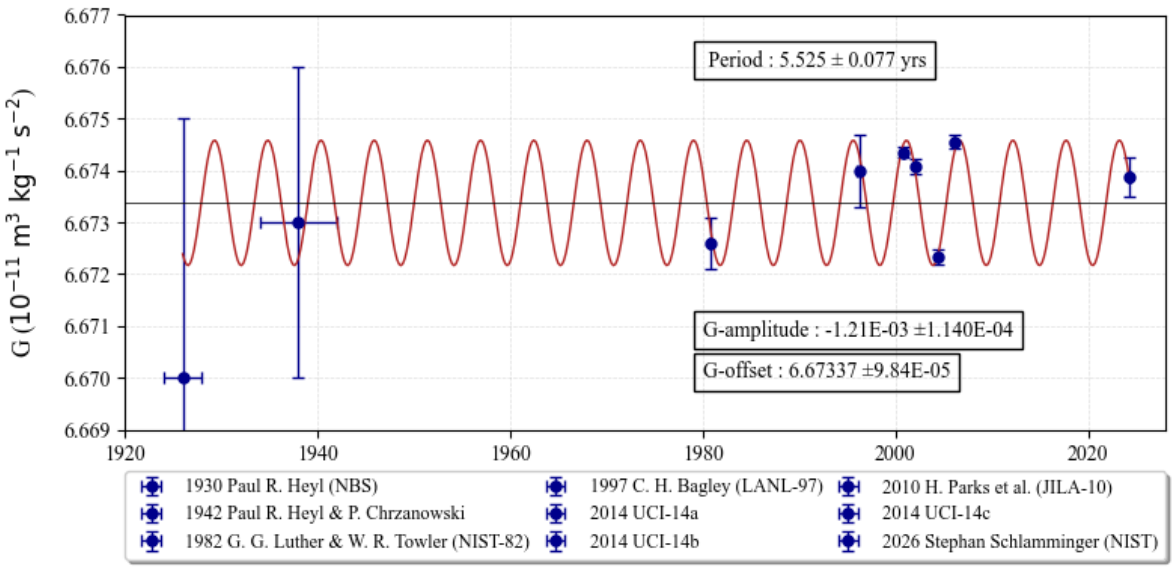

Figure 3: Data from USA-based experiments (1930 – 2026)

Geomagnetic Field under the PVN Charge Dynamo Mechanism

The mass-charge interaction naturally arises in the 4-D complex space when applying first principles to the equilibrium of net charge and net mass densities. In electromagnetic interactions, the charge corresponding to physical mass is defined as a primitive virtual negative (PVN) charge, expressed as $m[\mathrm{kg}] \sim -10^{-19} q[\mathrm{C}]$. Gravitational interaction is not independent of electromagnetism; consequently, gravity cannot be entirely isolated, as electromagnetic interference is an inherent and unavoidable part of reality. This interdependence suggests that variations in measured G values should correlate with fluctuations in the geomagnetic field.

Regarding Earth's magnetic field, it has been hypothesized that field generation is driven by internal electric charge separation caused by the magnetic force arising from the planet's rotation and its magnetic field. Under this hypothesis, negative charges accumulate beneath the crust, lithosphere and at the top of the asthenosphere, while an equal amount of positive charge resides in the uppermost layer of the outer core. (Kim 2008, 2025)

The PVN charge dynamo mechanism for geomagnetic filed can be applied for stellar objects in general. Since stellar objects have PVN charges corresponding to their mass, they interact with the internal charge distributions of other stellar objects. This means that stellar objects interact with each other's magnetic fields. For example, the solar magnetic field and its approximately 11-year flipping cycle can be explained by the PVN charges of the planets Jupiter and Saturn interacting with the Sun (Kim 2020), where we found that the strength of this interaction is periodic with a cycle of roughly 60 years due to their revolving periods. Interestingly, the same period is observed in the variation of the geomagnetic field.

Next, we investigate the sub-decadal variations in the geomagnetic field, which may correlate with changes in both the Length of Day (LOD) and the measured values of G. First, space charge density co-varies with the sunspot number cycle; conversely, atmospheric charge density and electrical conductivity exhibit an inverse correlation. From the perspective of the global electric circuit (GEC), Earth and its atmosphere are modeled as a massive spherical capacitor, where the ionosphere serves as the positive plate and Earth's crust acts as the negative plate. However, while variations in space charge density and solar magnetic storms during solar cycles can induce temporary disturbances in the geomagnetic field, they are incapable of producing a stable periodic pattern such as a 5.9-year cycle. Instead, such periodic variations in the geomagnetic field may be driven by the PVN charges of solar system planets.

Earth's Interior Charge Distributions with Interaction with Jupiter

When comparing PVN charges across the solar system, the Sun's charge is so immense that those of the planets can be ignored; however, it is thought that its effects on solar planets are shielded by the highly concentrated charged particles surrounding the Sun. The distribution of these charged particles is not isotropic; instead, a higher density is expected along the paths toward the planets, depending on the magnitude of their PVN charges and their distances from the Sun. Nevertheless, Earth is supposedly still under the influence of the Sun; solar activities generate a vast number of charged particles, the amount of which varies with sunspot numbers during a solar cycle. The shielding by those charged particles supposedly also affects the interaction between solar planets and Earth, which means, for example, that the strength of interaction from Jupiter or the Jupiter-Saturn system is reduced with increased solar activities.

This suggests the existence of either a deep valley within a single interaction period or two distinct interaction periods for Jupiter or the Jupiter-Saturn system, implying that the solar cycle is closely linked to variations in Earth's geomagnetic field.

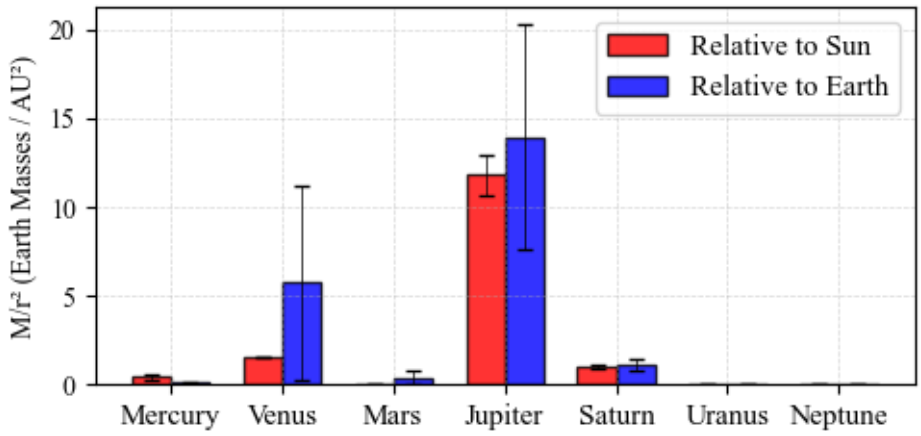

Figure 4: PVN charge interaction measures of solar planets

The strength of the PVN charge interaction between Earth and the other planets in the solar system is proportional to their masses and inversely proportional to the square of the distance (r) between them. Jupiter is the second-most massive object in the solar system. As shown in

Figure 4, the strength of Jupiter's PVN charge interaction with both Earth and the Sun dominates over all others; however, from a geocentric perspective, the interaction strength of Venus is particularly distinct. Figure 5 illustrates the distance variations between the Sun and Jupiter (11.86-year cycles), Earth and Jupiter (399-day cycles), and Earth and Venus (584-days cycles). As shown in Figure 4, the interaction strength between Earth and Jupiter varies significantly compared to that between the Sun and Jupiter; this is because the distance between Earth and Jupiter changes as Earth revolves around the Sun, as illustrated in Figure 5.

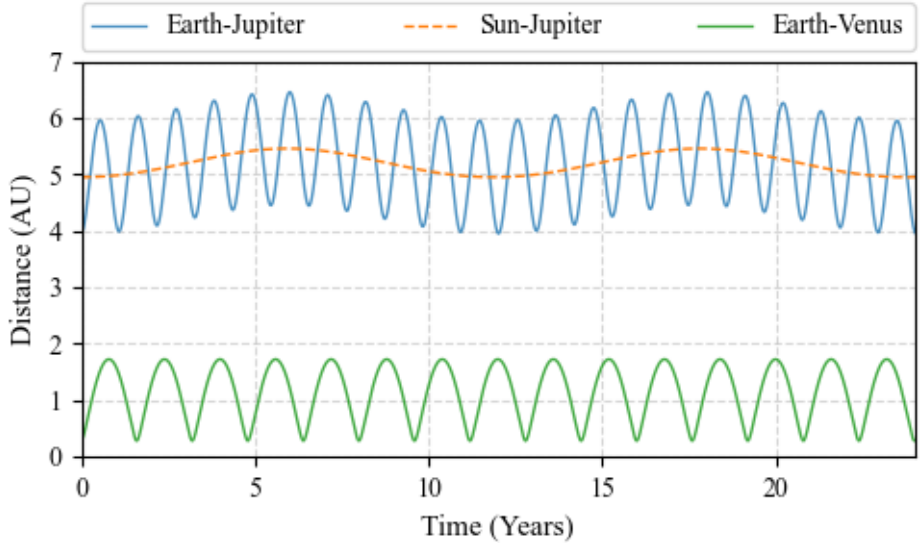

Figure 5: Distances (AU) vs. Time (Years)[§]

Its PVN charge interaction with Earth's interior charges—specifically the negative charge distribution beneath the crust—causes negative charges on the planet facing front side to be pushed down and those on the rear side to be pulled out. This creates a variation of charge distribution beneath the crust: As a possible scenario, let's say that on the front side, the negative charge distribution moves to $r \to r - \Delta_1$, while on the rear side, it moves to $r \to r + \Delta_2$, where r is the distance from the center of Earth. However, the distance variation Δ_2 on the rear side can be bigger than the Δ_1 on the front side because it is probably easier to move outward underneath the rigid lithosphere than to move into the inner hot asthenosphere. This creates the effect of an increase in negative charge density, which results in a current that increases with Earth's rotation.

Considering the geomagnetic field as explained above—generated by the negative charge distribution beneath the crust and Earth's rotation—any variation the negative charge distribution beneath the crust directly impacts the geomagnetic field. However, according to Faraday's law of induction, the resulting electromotive force (EMF) acts inversely to these geomagnetic variations. In short, the total variation of the geomagnetic field is driven by two combined factors: the changing negative charge distribution beneath the crust and the opposing

[§] AI generates the plot in response to the request, "Plot the distance vs. time among Earth and Jupiter, Earth and Venus, and Earth and the Sun."

EMF described by Faraday's law of induction. The basic mechanism of how variations in the geomagnetic field and length of day (LOD) correlate with changes in the negative charge distribution beneath the crust is explained in Appendix B.

Based on the PVN charge dynamo model for Earth's magnetic field (Kim 2025), variations in measured G values should correlate with changes in the geomagnetic field and LOD, as it is impossible to completely isolate gravity from electromagnetism.

As shown in Figure 5, the interaction strength of Jupiter's PVN charge oscillates annually due to Earth's orbit around the Sun, and these oscillations vary with Jupiter's orbital period around the Sun. However, the strength of this interaction is supposed to be modulated by solar cycles: because the Sun ejects a massive amount of charged particles, the interaction strength decreases depending on the stage of the solar cycle.

We can now propose an explanation for the long-standing "ugly duckling" issue in gravitational constant (G) measurements based on variations in the geomagnetic field, which occur due to Jupiter's PVN charge interaction. The annual fluctuation of the geomagnetic field accounts for the large uncertainties observed in G measurements, while its global variation—tied to Jupiter's orbital period—produces the periodic variation in the measured G values. In addition, when the interaction strength is divided by the solar maximum (the peak emission period of solar charged particles), the induced electric charge density beneath Earth's crust can exhibit a 5.9-year period (source for the variations in Appendix B), which is half of Jupiter's orbital period around the Sun.

Discussion

The measured values of the gravitational constant (G) are subject to electromagnetic interference because physical mass itself possesses electric properties, however small. Therefore, G is generally not independent of variations in the geomagnetic field and the length of day (LOD). However, to minimize interference from electromagnetic fields, we might consider placing the apparatus in a perfectly electrically conducting environment and performing static measurements.

Since these periodic variations in the geomagnetic field and the Earth's length of day (LOD) are believed to be driven not by the Earth's internal processes, but by periodic planetary interactions within the solar system, it is compelling to identify these signals within geomagnetic data and map them to specific celestial bodies. For instance, it would be fascinating to uncover the underlying mechanisms behind geomagnetic jerks, which are traditionally categorized as irregular phenomena occurring every 3 to 12 years.

Whether the CODATA 2026 recommended value of G will align closely with $6.6740 \times 10^{-11} \mathrm{m}^3\mathrm{kg}^{-1}\mathrm{s}^{-2}$ (as shown in Figure 2) remains an open question. Even if it does, we must ensure this alignment is not because G is changing over time, but rather because we have not yet resolved the hidden uncertainties and external interferences affecting G measurements.

Works Cited

Anderson, J. D., G. Schubert, V. Trimble, and M. R. Feldman. 2015. "Measurements of Newton's gravitational constant and the length of day." *EPL* 110 : 10002.

CODATA. . https://www.nist.gov/publications/codata-recommended-values-fundamental-physical-constants-2018.

Gershteyn, Mikhail L., Lev I. Gershteyn, Arkady Gershteyn, and Oleg V. Karagioz. 2002. "Experimental evidence that the gravitational constant varies with orientation." *arXiv.org e-print archive.* April 12. https://arxiv.org/pdf/physics/0202058.

Guynn, Preston. 2021. "Jupiter's Orbit and Alignment Relative to the Galaxy is the Physical Basis of Periodic Variations of Gravitational Constant G and the Length of Day." *viXra.org e-print achive.* November 14. https://vixra.org/pdf/2111.0073v1.pdf.

Johnston, Hamish. 2018. "Gravitational -constant mystery deepens with new precision measurements." *physicsworld.* Aug. 30. ttps://physicsworld.com/a/gravitational-constant-mystery-deepens-with-new-precision-measurements/.

Karagioz, O.V., and P.V. Izmailov. 2001. *Newtonian Constant of Gravitation G.* TRIBOTECH Research and Development Company. June 15. Accessed 09 2062. http://www.wdcb.ru/sep/GravConst/table_1.html.

Kim, Kiyoung. 2025. "Gravity in Earth's Interior and Geophysics." *viXra.org e-print archive.* July. https://vixra.org/pdf/2507.0067v1.pdf.

—. 2008. "Primitive Virtual Negative Charge." *arXiv.org e-print archive.* arxiv.org. November. https://arxiv.org/pdf/0811.0522.

—. 2020. "Solar Magnetic Field and the Dynamo Process." *viXra.org e-print archive.* November. https://vixra.org/pdf/2011.0087v1.pdf.

NIST. 2026. "NIST Weighs In on the Mystery of the Gravitational Constant." *NIST.* May 5. https://www.nist.gov/news-events/news/2026/04/nist-weighs-mystery-gravitational-constant.

physicsworld. 2001. "Helping 'big G' get back on track." *physicsworld.* Aug. 03. https://physicsworld.com/a/helping-big-g-get-back-on-track/.

Schlamminger, Stephan, J. H. Gundlach, and R. D. Newman. 2015. "Recent measurements of the gravitational constant as a function of time." *Physical Review D*, June.

Schlamminger, Stephan, Leon Chao, Craig Shakarji, Antonio Possolo, David Newell, Julian Stirling, Robert Cochrane, and Clive Speake. 2026. "Redetermination of the gravitational constant with the BIPM torsion balance at NIST." *Metrologia* 63 025012.

Unnikrishnan, C. S. . "Possible gravitational link between the 5.9 year period in the length of the day of the Earth and the 11.86 year orbit of Jupiter around the Sun." *Academia* 5.

Wikipedia. . "Gravitational Constant (G)." *Wikipedia.* https://en.wikipedia.org/wiki/Gravitational_constant.

Xue, Chao, Jian-Ping Liu, Qing Li, Jun-Fei Wu, Sharn-Qing Yang, Qi Liu, Cheng-Gang Shao, Liang-Cheng Tu, Zhong-Kun Hu, and Jun Luo. 2020. "Precision measurement of the Newtonian gravitational constant." *National Science Review* 7: 1803 - 1817.

Appendix A

	Year	Research	$G \times 10^{11}$ (SI)	±Error	Measurements	decimal Year	Y-error	ΔYears	Ref.
1	1930	Paul R. Heyl (NBS)	6.67	0.005	(1924 -1928)	1926	2	4	Wikipedia
2	1942	Paul R. Heyl & P. Chrzanowski	6.673	0.003	(1934 - 1942)	1938	4	4	Wikipedia
3	1972	C. Pontikis et al.	6.6714	0.0006	1971	1971.5	0.5	0.5	AI Search
4	1979	Marat U. Sagitov et al.	6.6745	0.0008	(03/1795 – 01/1798)	1976.42	1.42	2.58	AI Search
5	1982	G. G. Luther & W. R. Towler (NIST-82)	6.6726	0.0005	08/29/1980 - 10/10/1980	1980.71	0.05	1.29	NIST PMC
6	1997	C. H. Bagley (LANL-97)	6.674	0.0007	01/01/96 - ? 05/31/96	1996.2	0.2	0.8	NIST PMC
7	2005	HUST-05	6.6723	0.0009	08/04/1997 - 10/15/1997	1997.68	0.09	7.32	NIST PMC
8	1999	Mark P. Fitzgerald et al. (MSL)	6.6742	0.0007	1998	1998.5	0.25	0.5	IOP
9	2000	Jens H. Gundlach (Univ. of Wash.) (UW-00)	6.674215	0.000092	03/10/2000 - 04/18/2000	2000.24	0.05	0.24	NASA Goddard
10	2001	T. J. Quinn et al. (BIPM / NIST)	6.67565	0.00045	03/21/2002 - 11/01/2002	2000.52	0.3	0.48	NIST PMC
11	2001	T. J. Quinn et al. (BIPM / NIST)	6.67553	0.0004	09/29/2000 - 11/02/2000	2000.79	0.004	0.21	NIST PMC
12	2014	UCI-14a	6.67435	0.0001	10/04/2000 - 11/11/2000	2000.81	0.05	13.19	NIST PMC
13	2001	T. J. Quinn et al. (BIPM/ NIST)	6.67559	0.00027	09/29/2000 - 12/13/2000	2000.84	0.1	0.16	NIST PMC
14	2002	UWUP-02	6.667422	0.00098	01/12/2001 - 06/29/2001	2001.26	0.23	0.74	NIST PMC
15	2006	S. Schlamminger et al. (Univ. of Zurich) (UZH-06)	6.674252	0.00012	07/31/2001 - 09/09/2001	2001.63	0.05	4.37	NIST PMC
16	2001	J. Schurr et al. (University of Zurich)	6.67554	0.00016	08/2001 – 09/2001	2001.66	0.004	0.66	NIST_1
17	2014	UCI-14b	6.67408	0.00015	03/25/2002 - 05/12/2002	2002.06	0.06	11.94	NIST PMC
18	2003	T.R. Armstrong et al. (MSL-03)	6.67387	0.00027	03/21/2002 - 11/01/2002	2002.52	0.3	0.48	NIST PMC
19	2007	B.J. Fixler et al.	6.693	0.034	(2002 -2006)	2004	2	3	PMC_1
20	2010	H. Parks et al. (JILA-10)	6.67234	0.00014	05/12/2004 - 06/06/2004	2004.39	0.03	5.61	NIST PMC
21	2014	UCI-14c	6.67455	0.00013	04/08/2006 - 05/14/2006	2006.04	0.04	7.96	NIST PMC
22	2009	Luo Jun et al. (Huazhong Univ. HUST)	6.67352	0.00019	03/21/2007 - 05/20/2007	2007.29	0.08	1.71	NIST PMC
23	2013	T. J. Quinn et al. (BIPM-13c)	6.67586	0.00036	08/31/2007 - 09/10/2007	2007.67	0.01	5.33	NIST PMC
24	2013	T. J. Quinn et al. (BIPM-13sc)	6.67554	0.00016	08/31/2007 - 01/16/2008	2007.85	0.18	5.15	NIST PMC
25	2013	T. J. Quinn et al. (BIPM-13s)	6.67515	0.00041	11/08/2007 - 01/16/2008	2007.93	0.08	5.07	NIST PMC
26	2010	Tu L. -C et al.	6.67346	0.00021	10/08/2008 – 11/30/2008	2008.84	0.07	1.16	NIST PMC
27	2014	G. Rosi et al. (LENS-14)	6.67191	0.00099	07/05/2013 – 07/12/2013	2013.5	0	0.5	NIST PMC
28	2018	Qing Li (Huazhong Univ. Sci & Tech)	6.674184	0.000078	12/10/2016 - 02/27/2017	2017.05	0.1	0.95	PMC
29	2018	Chao Xue (Huazhong Univ. Sci & Tech)	6.674484	0.000078	02/14/2017 - 04/28/2017	2017.22	0.1	0.78	PMC
30	2022	T. Westphal et al.	6.04	0.06	(2019 – 2020)	2019.5	0.5	3	arXiv
31	2026	Stephan Schlamminger (NIST)	6.67387	0.00038	01/24/2024 - 06/22/2024	2024.26	0.2	1.74	NIST_2

Table A: Gravitational constant G measurements (1930 – 2026)

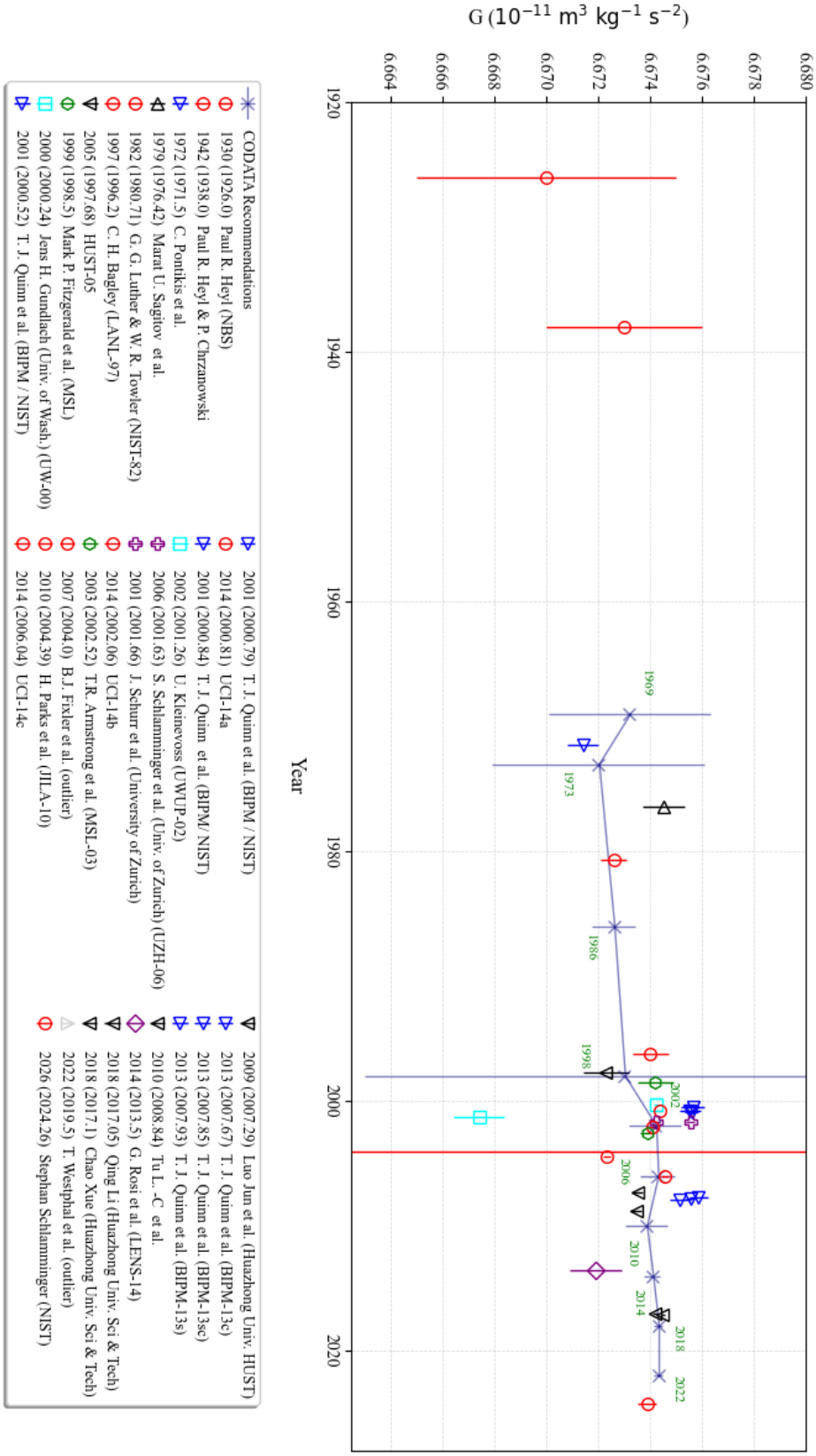

Figure A: Gravitational Constant Timeline (1930 -2026)

Table A lists the gravitational constant (G) values measured in laboratory experiments worldwide from 1930 to 2026. The dataset includes the following parameters: **Year** (publication year); **Research** (primary researcher or research ID); **Big G** (measured (G) values); **Error** (absolute uncertainty); **Measurements** (time measurements); **decimal Year** (midpoint of the measurement time); **Y-error** (corresponding error); **Δ Years** (years delayed for publication); and **Ref** (reference).

The list is sorted in sequence by decimal Year and shown in Figure A, in which markers and their colors are corresponded to their nationalities (indicating different locations in the experiments). In addition, G values recommended from CODATA (Committee on Data of International Science Council) are included. (Wikipedia; Xue, et al. 2020; Schlamminger, Gundlach and Newman, 2015; CODATA)

Appendix B

The Earth's main magnetic field is explained using the PVN charge dynamo mechanism. Under this mechanism (Kim 2008), the negative charge distribution that generates the main geomagnetic field is concentrated toward the Earth's equator. When external forces interfere with this charge distribution, we expect geomagnetic field changes and variations in the Length of Day (LOD) due to Faraday's law of induction. The following two simple cases illustrate how this mechanism works and estimate the scale of these changes.

Case 1:

Let us make a simple approximation by assuming a uniform charge density σ on the surface of Earth, modeled as a sphere of radius R. If the sphere rotates with an angular velocity ω, the resulting magnetic dipole moment $\mathcal{M}$ is given by

$$\mathcal{M} = \frac{4}{3}\pi\sigma R^4\omega \tag{A1}$$

Magnetic field inside, $\vec{B}_{in} = \frac{2}{3}\mu_0\sigma R\omega\,\hat{z}_1$; outside, $\vec{B}_{out} = \frac{\mu_0\sigma R^4\omega}{3r^2}\left[2\cos(\theta)\,\hat{r}_1 + \sin(\theta)\,\hat{\theta}_1\right]$.

If the surface charge density changes, a torque is generated according to Faraday's law of induction as

$$N = -\frac{8}{9}\pi\mu_0 R^5\sigma\dot{\sigma}\,\omega \tag{A2}$$

In axial direction ($\hat{z}$). Since $N = I_{\mathrm{m}}\dot{\omega}$ where I_{m} is the moment of inertia of the system. Substituting this into Eq. (A2) yields

$$\frac{\dot{\omega}}{\omega} = -\frac{2}{3}\frac{\mu_0 R^2\mathbb{V}}{I_{\mathrm{m}}}\,\sigma\dot{\sigma} \tag{A3}$$

where $\mathbb{V} = \frac{4}{3}\pi R^3$. If $\beta = \frac{1}{3}\mu_0 R^2\mathbb{V}/I_{\mathrm{m}}$, the relation of angular velocity ω to the surface charge density σ is

$$\omega(t) = \omega_0\, e^{-\beta(\sigma^2-\sigma_0{}^2)} \tag{A4}$$

If $\beta \ll 1$ and $\sigma = \sigma_0(1+\epsilon)$, Eq. (A4) simplifies to

$$\frac{T}{T_0} = 1 + 2\epsilon\beta\sigma_0$$

For Earth's magnetic dipole moment, $\mathcal{M}_{\oplus}\sim 8\times 10^{22}$ A·m^2, the surface charge density $\sigma\sim 0.16$ C·m^{-2} with Eq. (A1), and $\beta\sim 2.3\times 10^{-10}$ with Earth's moment of inertia $I_{\oplus}\sim 8\times 10^{37}$. If $\epsilon\sim 10^{-2}$, It results in $\Delta T\sim 6.3\times 10^{-8}$ s.

Case 2:

let's make a simple approximation assuming a line charge density λ on the equator of Earth, which generates a magnetic dipole moment as $\mathcal{M} = \pi R^2 \cdot \lambda V$ with Earth's rotation, where R is Earth's radius and V is tangential velocity at the equator. Magnetic field at the center of the loop made by the charge distribution,

$$\vec{B} = \frac{\mu_0 I}{2R}\ \hat{z} \tag{A5}$$

where $I = \lambda V$. If the line charge density (λ) changes, the velocity (V) must also change due to Faraday's law of induction,

$$-\frac{\partial \vec{B}}{\partial t} = \nabla \times \vec{E}$$

If the average $\vec{B}$ field intensity inside the loop in the axial direction $(\hat{z})$ is given as

$$\langle B \rangle = \frac{\mu_0 I}{2R} \cdot \mathrm{C_{av}} \tag{A6}$$

in which $\mathrm{C_{av}} \sim 10^1$. According to Faraday's law of induction, $\pi R^2 \langle \dot{B} \rangle = -2\pi R \cdot E$, where the induced electric field E generates a reactive force on the charges given by $F = 2\pi R\lambda \cdot E$. This result in a torque $N = R \cdot F$ in the axial direction $(\hat{z})$, which can be expressed in terms of the moment of inertia of the system (I_m) as

$$I_\mathrm{m}\dot{\omega} = -\pi\lambda R^3 \langle \dot{B} \rangle$$

To simplify the problem, let us assume that the electrical conductivity in the medium around the charge distribution is zero. That is,

$$-\frac{I_\mathrm{m}}{\pi\lambda R^4}\ \dot{V} = \frac{\mathrm{C_{av}}\ \mu_0}{2R}\left(\dot{\lambda}\, V + \lambda\, \dot{V}\right)$$

$$-\frac{\dot{V}}{V} = \frac{\lambda\, \dot{\lambda}}{\left[\frac{2I_\mathrm{m}}{\mathrm{C_{av}}\ \mu_0 \cdot \pi R^3} + \lambda^2\right]}$$

Let's say $L \equiv \frac{2I_\mathrm{m}}{\mathrm{C_{av}}\mu_0 \cdot \pi R^3} \sim \frac{I_m}{5\times 10^{15}}$, it can be simplified as

$$\frac{V}{V_0} = \sqrt{\frac{L + {\lambda_0}^2}{L + \lambda^2}}$$

where V_0 is the initial velocity, and λ_0 is the initial charge density on the loop. Since $V = R\omega$ (where $\omega = 2\pi/T$),

$$\frac{T}{T_0} = \sqrt{\frac{1+\frac{\lambda^2}{L}}{1+\frac{{\lambda_0}^2}{L}}} \tag{A7}$$

If $\lambda^2/L \ll 1$ and $\lambda = \lambda_0(1+\epsilon)$, where $\epsilon \ll 1$, the variation of Length of Day (LOD) of Earth can be estimated as

$$\frac{T}{T_0} \cong 1 + \epsilon\frac{{\lambda_0}^2}{L} \tag{A8}$$

And the variation of magnetic field also can be estimated as

$$\frac{B}{B_0} \cong 1 + \varepsilon \tag{A9}$$

Now, let us consider the magnetic dipole moment of Earth's magnetic field, which is $\mathcal{M} \sim 8 \times 10^{22}$ (A·m^2). If this is applied to the loop current described above, the corresponding line charge density $\lambda_0 \sim \frac{\mathcal{M}}{\pi R^2 V_0} = 1.3 \times 10^6$ (C·m^{-1}), where tangential velocity at the equator $V_0 \sim 465$ m/s. Considering Earth's moment of inertia, $I_m \sim 8 \times 10^{37}$ (kg m^2), we find that $L \sim 1.6 \times 10^{22}$ and ${\lambda_0}^2/L \sim 1.0 \times 10^{-10}$, which seems to be small because $\Delta T \sim 10^{-3}$ s has been reported.

However, to be realistic we can adjust λ_0 based on the condition of the magnetic field intensity at the Magnetic North Pole, $B \sim 6 \times 10^{-5}$ T, which yields $\lambda_0 \sim 3.7 \times 10^6$. In addition, the Earth's moment of inertia (I_m) must be considered; because the Earth's core does not respond instantly to an external torque but is instead dragged, this results in an effective moment of inertia, $I_\mathrm{eff} \sim 7.1 \times 10^{37}$kg·m^2. Now, if we consider ${\lambda_0}^2/L \sim 1.0 \times 10^{-9}$ with $\epsilon \sim 10^{-2}$, $\Delta B/B_0 \sim 10^{-2}$ and $\Delta T \sim 10^{-6}$ s, the resulting value is still too small.

A possible scenario is as follows: if a sudden, high-frequency external torque is applied to the Earth for a very short duration, and everything below the crust completely fails to respond, the effective moment of inertia will drop dramatically to approximately $I_\mathrm{eff} \sim 7 \times 10^{35}$ kg·m^2. This is only about 0.9% of the Earth's total rotational inertia ($I_\oplus \sim 8 \times 10^{37}$ kg·m^2). While this seems unrealistic, it cannot be dismissed as nonsense when considering the explanation of plate tectonics under the PVN charge dynamo mechanism (Kim 2025). Hence, treating this as a limiting case, if $I_\mathrm{eff} \sim 7 \times 10^{35}$ kg·m^2, then $\Delta T \sim 10^{-4}$ s. On the other hand, this corresponds to $\Delta T \sim 7 \times 10^{-6}$ s in Case 1.

Source for the variations

As shown in Figure 4, the charge density variation beneath Earth's crust can include planetary influences from Jupiter, Venus, and Saturn; however, these influences are presumed to be modulated by solar activity that generates massive amounts of charged particles. Specifically, the influence from Venus (an inner planet near the Sun) should be weakened by a solar shielding

effect. Similarly, Jupiter's fluctuating influence— driven by Earth's annual orbit around the Sun (Figure 5)—should also be reduced. Furthermore, two interference patterns separated near the solar maximum are expected.

Let the charge density, $\lambda(t)$, which represents a change in the charge distribution beneath the crust, be approximated as

$$\lambda(t) \approx \lambda_0 \{1 + a_1 \sin[\omega_s(t - t_1)] + a_2 \sin[2\omega_s(t - t_2)] + a_{12} \sin[12\omega_s(t - t_{12})]\}$$

where $\omega_s = 2\pi/T_J$ and the coefficients satisfy $a_1, a_2,$ and $a_{12} \ll 1$. Here, T_J represents Jupiter's orbital period around the Sun. As demonstrated in Case 1 and Case 2, the periods appearing in the variations of both the geomagnetic field and the length of day (LOD) match the period of the underlying charge density source.